Journal of information and
communication convergence engineering
http://jicce.org

J. Inf. Commun. Converg. Eng. 20(4): 303-308, Dec. 2022 Regular paper

ResNet-Based Simulations for a Heat-Transfer Model Involving an Imperfect Contact

Guangxing Wang[1], Gwanghyun Jo[2*], and Seong-Yoon Shin[3*], ***Member, KIICE***

[1]Computer and Big Data Science, JiuJiang University, Jiujiang 332005, China
[2]Department of Mathematics, Kunsan National University, Gunsan 54150, Republic of Korea
[3]School of Computer Information & Communication Engineering, Kunsan National University, Gunsan 54150, Republic of Korea

Abstract

Simulating the heat transfer in a composite material is an important topic in material science. Difficulties arise from the fact that adjacent materials cannot match perfectly, resulting in discontinuity in the temperature variables. Although there have been several numerical methods for solving the heat-transfer problem in imperfect contact conditions, the methods known so far are complicated to implement, and the computational times are non-negligible. In this study, we developed a ResNet-type deep neural network for simulating a heat transfer model in a composite material. To train the neural network, we generated datasets by numerically solving the heat-transfer equations with Kapitza thermal resistance conditions. Because datasets involve various configurations of composite materials, our neural networks are robust to the shapes of material-material interfaces. Our algorithm can predict the thermal behavior in real time once the networks are trained. The performance of the proposed neural networks is documented, where the root mean square error (RMSE) and mean absolute error (MAE) are below 2.47E-6, and 7.00E-4, respectively.

Index Terms: Composite material, deep learning, heat transfer, Kapitza thermal resistance, ResNet

I. INTRODUCTION

Heat transfer in composite media has been studied extensively because of its importance in material science (see [1, 2] and the references therein). If the interfaces of the adjacent materials are in perfect contact, both the temperature and flux variables are continuously matched along the material interfaces. However, it is difficult to expect perfectly matched conditions in practice, that is, in the presence of gaps between the contacting domains, the temperatures are discontinuous across the material interfaces. Kapitza [3] modelled jump conditions for imperfect contact where temperature jumps appear across the interface, the amounts of which are affected by the Kapitza thermal resistance.

There have been various attempts to solve thermal transfer problems involving imperfect conditions using finite element methods (FEMs), see [4-6]. However, these methods are rather complicated because the Kapitza-type interface conditions must be carefully treated. In addition, simulations of the heat transfer in composite materials cannot be obtained in real time by FEM-based algorithms.

However, there have been huge developments in deep learning (DL) communities (see [7-12] and the references therein). One of the main advantages of DL-based methods is that once the networks are trained, they can produce predictions of the target variable in real time.

Received 12 October 2022, **Revised** 13 October 2022, **Accepted** 05 November 2022
***Corresponding Authors** Gwanghyun Jo (E-mail: gwanghyun@kunsan.ac.kr, Tel: +82-63-469-4542)
Department of Mathematics, Kunsan National University, Gunsan 54150, Republic of Korea
Seong-Yoon Shin (E-mail: s3397220@kunsan.ac.kr, Tel: +82-63-469-4860)
School of Computer Information & Communication Engineering, Kunsan National University, Gunsan 54150, Republic of Korea

Open Access **https://doi.org/10.56977/jicce.2022.20.4.303** print ISSN: 2234-8255 online ISSN: 2234-8883

In this study, we developed a DL-based thermal simulation for a composite material. One good aspect of the artificial neural network (ANN)-based approach is that one can expect real-time thermal conduction simulation once the networks are trained. This is in contrast to conventional FEM-based methods, whose computation times are non-negligible. Another advantage of the proposed DL-based algorithms is that they are robust with respect to the geometry of the material-material interface. In fact, the inputs of the proposed DL architectures are material-material interfaces. Once the geometrical contribution of a composite material is substituted into the algorithm, the desired prediction of the target variable (i.e., temperature) can be obtained in real time. This method of obtaining solutions is more user-friendly compared to FEM-based approaches.

To train the neural networks, we produced datasets by numerically solving the heat equations for various configurations of composite material shapes. Here, the immersed finite element method (IFEM) [13] was used as the numerical method. For the architecture of the DL, we employed ResNet-type [7] structures, where so-called ResBlocks with identity maps are repeated several times. With the presence of identity-maps in ResBlocks, one can avoid the "gradient-vanishing" phenomenon even with a large number of layers.

The remainder of this paper is organized as follows. The model equation and the derivation of its weak form are presented in the next section. ResNet-based neural networks are developed in Section 3. The next section reports the performance of ResNet-based neural networks in predicting the solutions of heat-transfer models involving composite materials. Finally, we present our conclusions in the last section.

II. MODEL EQUATION AND DERIVATION OF ITS WEAK FORM

In this section, the governing equation of the model and its derivation of a weak form are described. Consider a composite material $\Omega \subset R^2$ having two parts $\Omega = \Omega_1 \cup \Omega_2$ where Ω_2 is imbedded in Ω. Here, denote Γ to be the material interface dividing Ω_1 and Ω_2. The governing equation for the heat transfer model involving the Kapitza interface condition with a Kapitza thermal resistance α is as follows:

$$\begin{cases} \boldsymbol{q_i} = -k_i \nabla T_i, \quad in\ \Omega_i, i = 1,2, & (1) \\ \nabla \cdot \boldsymbol{q_i} = f, \quad in\ \Omega_i, i = 1,2, & (2) \\ [T]_\Gamma = -\alpha \boldsymbol{q_2} \cdot \boldsymbol{n_2}, & (3) \\ [\boldsymbol{q} \cdot \boldsymbol{n}_\Gamma]_\Gamma = 0, & (4) \\ T = g, \quad in\ \partial\Omega, & (5) \end{cases}$$

where $\boldsymbol{n}_i$s are the outward unit normal vector to Ω_i ($i = 1, 2$) and $\boldsymbol{n}_\Gamma = \boldsymbol{n}_1$. Here, $[\cdot]_\Gamma$ implies a jump of functions across the interface, that is, $[T]_\Gamma = T_1 - T_2$ and $[\boldsymbol{q} \cdot \boldsymbol{n}_\Gamma]_\Gamma = \boldsymbol{q}_1 \cdot \boldsymbol{n}_\Gamma - \boldsymbol{q}_2 \cdot \boldsymbol{n}_\Gamma$. Equations (1) and (2) relate the temperature (T) and heat (q) variables by using Fick's law. Eqs. (3) and (4) describe the Kapitza interface conditions [3]. Finally, (5) describes the boundary conditions. The temperature variable in a composite material can be determined by solving Eqs. (1)-(5).

The weak problem for (1)-(5) can be derived as follows: For convenience, we assume that $g = 0$ in Eq. (5). We need some notations. Let D be any domain in R^2 and $H^1(D)$ and $H_0^1(D)$ be the usual Sobolev space. Furthermore, the broken space is defined as follows:

$$\widetilde{H}_0^1 = \{v \in L^2(\Omega) \mid v \in H^1(\Omega^1) \cap H^1(\Omega^2)\ and\ v|_\Omega = 0\}.$$

By multiplying a function $v \in \widetilde{H}_0^1$ to (1) and (2) and by applying integration by parts in each subdomain, we have

$$\sum_i \left(\int_{\Omega_i} k_i \nabla T_i \cdot \nabla v \, dx - \int_{\partial\Omega_i} k_i \nabla T_i \cdot \boldsymbol{n}_i v \, ds \right) = \int_\Omega f v \, dx .$$

Here, using Kapitza interface conditions (3) and (4), the second term of the above equation is written as follows:

$$\sum_i - \int_{\partial\Omega_i} k_i \nabla T_i \cdot \boldsymbol{n}_i v \, ds = \int_\Gamma \left(-k^- \frac{\partial T^-}{\partial \boldsymbol{n}_\Gamma} + k^+ \frac{\partial T^+}{\partial \boldsymbol{n}_\Gamma} \right) v ds$$
$$= \int_\Gamma k^+ \frac{\partial T^+}{\partial \boldsymbol{n}_\Gamma} [v]_\Gamma ds = \int_\Gamma \frac{1}{\alpha} [T]_\Gamma [v]_\Gamma .$$

Summarizing the above equations, a weak problem for (1)-(5) is written as follows: find $T \in \widetilde{H}_0^1$ such that it satisfies

$$\int_{\Omega_1 \cup \Omega_2} k \nabla T \cdot \nabla v \, dx + \int_\Gamma \frac{1}{\alpha} [T]_\Gamma [v]_\Gamma = \int_\Omega f v \, dx , \quad \forall\, v \in \widetilde{H}_0^1. \tag{6}$$

Based on the weak problem (6), the IFEM is employed to generate datasets for training the ANN.

III. METHODS

In this section, we propose ANN-based simulation methods for heat-transfer models in composite materials. In particular, ResNet-based neural networks produce an approximation solution for the temperature variable in Eqs. (1)-(5). The remainder of this section is organized as follows. The IFEM for model Eqs. (1)-(5) is described in the first subsection. The ResNet-based networks for heat transfer are described in the following subsections.

A. Immersed Finite Element Methods Heat-Transfer Model

In this subsection, we propose the IFEM for heat equations involving imperfect contact conditions, based on [13]. Our version of the IFEM is similar to that of [13], but a different local space is employed. We briefly describe the methods as follows. (details of the derivations of discrete weak problems can be found in [13]).

Let $\mathcal{T}_h$ be a uniform triangulation of Ω by right triangles having an edge size h and let $\mathcal{F}_h$ be the set of edges of elements in $\mathcal{T}_h$. Let E be a typical element in $\mathcal{T}_h$ and let $S_h(E)$ be set of first order polynomials in E. Assume that E is cut through by Γ, so that $E = E_1 \cup E_2 := (E_1 \cap \Omega_1) \cup (E_2 \cap \Omega_2)$. Because the first-order polynomials in S_h(T) are continuous, they cannot satisfy Kapitza conditions (3) and (4). Hence, we modify a function $v \in S_h(E)$ to be a piecewise linear function $\hat{v}$ satisfying the Kapitza conditions, that is, $\hat{v}$ has the following form:

$$\mathrm{v}|_{E_1} = a_1 + b_1 x + c_1 y, \qquad v|_{E_2} = a_2 + b_2 x + c_2 y$$

and coefficients (a_1, b_1, c_1, a_2, b_2, c_3) are determined to satisfy Kapitza conditions as

$$\begin{cases} \hat{v}(X_i) = v(X_i), \quad i = 1,2,3, \\ [\hat{v}]_\Gamma = -\alpha k^+ \nabla\left(\hat{v}|_{T_2}\right) \cdot \boldsymbol{n}_2, \\ [k \nabla \hat{v} \cdot \boldsymbol{n}_\Gamma]_\Gamma = 0, \end{cases}$$

where X_i's are nodes of E. The set of modified functions $\hat{v}$ is defined as $\tilde{S}_h(T)$. Finally, the global finite element space $\tilde{S}_h(\Omega)$ is defined as a set of functions in $L^2(\Omega)$ satisfying:

$$\begin{cases} v|_T \in S_h(E), \quad if\ E\ is\ not\ cut\ through\ by\ \Gamma \\ v|_T \in \tilde{S}_h(E), \quad if\ E\ is\ cut\ through\ by\ \Gamma \\ v|_{E_s}(X) = v|_{Ew}(X), \quad where\ X\ is\ common\ nodes\ of\ E_s\ and\ E_w \\ v(X) = 0, \quad if\ X\ is\ on\ \partial\Omega. \end{cases}$$

We are now in a position to state IFEM for model equations (1)-(5): find $T_h \in \tilde{S}_h(\Omega)$ satisfying

$$\begin{aligned} \sum_{E \in \mathcal{T}_h} \int_E k \nabla T_h \cdot \nabla v_h \mathrm{ds} &+ \int_\Gamma \frac{1}{\alpha} [T_h]_e [v_h]_\mathrm{e} \mathrm{ds} \\ &- \sum_{e \in \mathcal{T}_h} \int_e \{k \nabla T_h \cdot \boldsymbol{n}_e\}_e [v_h]_\mathrm{e} \mathrm{ds} \\ &- \sum_{e \in \mathcal{T}_h} \int_e \{k \nabla v_h \cdot \boldsymbol{n}_e\}_e [T_h]_\mathrm{e} \mathrm{ds} \\ &+ \sum_{e \in \mathcal{T}_h} \frac{\sigma}{|e|} \int_e [v_h]_e [T_h]_\mathrm{e} \mathrm{ds} \\ &= \int_\Omega f \mathrm{v_h}\, \mathrm{dx}, \end{aligned}$$

for all $v_h \in \tilde{S}_h(\Omega)$.

It was reported in [13] that numerical solutions obtained by the IFEM for robo-interface condition elliptic partial differential equations have optimal error convergences, that is, as the mesh size is halved L^2-errors are reduced by 1/4 and H^1-errors are reduced by 1/2. Although this is not the scope of this work, similar error convergences were observed for the IFEM defined in (7), implying that IFEM-generated solutions can be used as reference solutions for a heat-transfer model in a composite material.

B. ResNet-based Neural Networks for Heat-Transfer in a Composite Material

In this subsection, ResNet-based neural networks are developed to predict the solutions (temperature variables) of heat transfer in a composite material. First, we explain the generation process of the datasets. We intend to develop ANNs that are robust with respect to the geometry of embedded materials. For this purpose, different interface shapes were considered, as shown in Fig. 1. Here, interfaces were created by perturbating circles using randomly chosen parameters c_1, c_2, θ_1, θ_2 as below

$$r = r_0(1 + c_1 \sin(\theta - \theta_1) + c_2 \sin(2(\theta - \theta_2))).$$

Here,Γ is chosen by level sets for r, i.e., $\Gamma = \{(x, y) \mid r(x, y) = 0\}$.

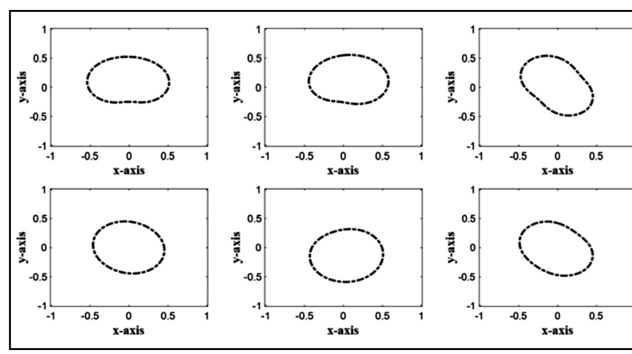

Fig. 1. Examples of geometry of embedded material. Interfaces separating material subdomains are drawn by dashed-lines.

The formatting of datasets of type (X_i, Y_i)'s ($i = 1$, ..., *nSamples*) are described. First, each X_i represents the shape of the material composite, that is, we set $X_i(x, y) = 1$ if (x, y) is located in Ω_1 and $X_i(x, y) = 0$ otherwise.Y_i is the point-wise value of T_h, that is, $Y_i(x, y) = T_h(x, y)$. As usual, Y_i is normalized such that the values of Y_i are between [0, 1]. The process of generating data is summarized below.

1) A two-dimensional input X_i is defined to represent the subdomains Ω_1 and Ω_2.
2) Next, by IFEM in (7), the numerical solution T_h is obtained.
3) Finally, by matching the point-wise values of T, a two-dimensional output Y_i which represents the solution of the heat equation is defined.

The remainder of this subsection is devoted to the development of ANNs for a heat-transfer model in a composite material. Because the imperfect contact Kapitza resistance model has discontinuous solutions, it requires a large number of network parameters. To avoid the so-called gradient-vanishing phenomenon for deep neural networks, ResNet-type networks [7], which accompany the concept of skip connections, were employed in this study.

We denote *CONV2D(kern=n,gen=m, stride=s)* as a typical convolutional layer with $n \times n$ size filters, m number of filters, and stride size s. The idea of the residual block (ResBlock) is to accompany an identity-map-type skip connection between the input and outputs, that is, the input (X) and output (Y) of ResBlock are related as

$$Y = F(X;\theta) + X$$

where $F(X;\ \theta) = (CONV2D \cdot \sigma \cdot CONV2D)(X)$ and σ is a nonlinear activation function. Because the differentiation of Y with respect to X always has identity maps, gradients of errors can be back-propagated by identity maps, which prevents the gradient-vanishing phenomenon. In this study, a RELU function was employed for the activation σ. For convenience, the following notation is used:

$$RESBLOCK(kern = n,\ gen = m) = (CONV2D(n,m,1) \cdot \sigma \cdot CONV2D(n,m,1))(X) + X.$$

Finally, a ResNet type neural network is proposed as below:

Algorithm. ResNet(*m, d*).
Suppose that input X is given. ResNet(*m, d*) was obtained using the following process:

1) Apply down-samplings.
 X = CONV2D(7,m,1)(X)→X = CONV2D(3,2m,2)(X)
 →X = CONV2D(3,4m,2)(X)
 →X = CONV2D(3,8m,2)(X)
2) Apply RESBLOCK *d*-times.
 for *i = 1,…, d*
 X = RESBLOCK(3, 8m)
 end for
3) Apply up-samplings.
 X = CONVT2D(3,4m,2)(X)
 →X = CONVT2D(3,2m,2)(X)
 →X = CONVT2D(3,m,2)(X)
 →ResNet(m, d) = *CONVT2D(7,1,1)(X)*

We note that at the down-sampling stage in the above algorithm, the resolution of the data is reduced while the number of kernels increases. Here, the total CPU time at the lower level does not increase even when the number of filters is doubled. In this manner, features at different resolutions can be effectively extracted. At the lowest level, RESBLOCK was applied *d*-times. Then, the feature maps were up-sampled using CONVT2D. In this algorithm, there are two control parameters m and d that affect the total number of parameters in ResNet(m,d). As m increased, the number of filters at each stage increased. However, as d increases, the number of layers in the networks increases. For the objective function, the mean square errors between the IFEM-generated and ResNet-generated solutions were used.

IV. EXPERIMENT AND RESULTS

In this section, we report the performance of ResNet(m,d) for heat transfer problems in composite materials. The domain is $\Omega = [-1, 1]^2$ and triangulation $\mathcal{T}_h$ is constructed by right-triangles of size $h = 2^{-6}$ resulting in 128×128 nodes. The Kapitza thermal resistance constant was set to $\alpha = 0.2$. As for the boundary condition, we set $g = 1$ on the left side of Ω and $g = 0$ on the right side of Ω. Also, a homogeneous source term is assumed, that is, $f = 0$ in (2). Note that our methods perform similarly for different parameter settings.

A dataset containing 10,000 IFEM generated solutions for the heat-transfer equations involving composite materials was used. Among these, 7000 samples were used for the training set, 1000 samples were used for the validation set, and 2000 samples were assigned to the test set. To train ResNet, an ADAM optimizer with a learning-rate parameter of 0.0002 was used for 200 epochs. ResNet(m,d), was implemented by Keras on an NVIDIA RTX 3090. To find the optimal parameters of ResNet(m,d), the usual root mean squared error (RMSE) and mean absolute error (MAE) of the test sets were compared for different cases of (m,d). Here, the errors between the solutions generated by ResNet(m,d) and the numerical solutions obtained by IFEM were computed.

Table 1 reports CPU time and accuracies of solutions obtained by ResNet(m,d). Both the CPU time and number of parameters increase as m or d increase. Among the various versions of ResNet(m,d) ResNet(*10,5*) produces solutions with the smallest RMSE and MAE. However, other choices result in reasonably small errors, that is., RMSEs are below 3E-6 and MAEs are below 7E-4 for all cases. Evolutions of RMSE and MAE with respect to increasing epoch numbers are plotted in Fig. 2 for the case of ResNet(10,5). Here, both RMSE and MAE are decreasing stably.

The temperature variables predicted by ResNet(10,5) for heat-transfer problems with different composite material shapes are plotted in Fig. 3. Here, it is observed that the temperatures are discontinuous near the material-material inter-

Table 1. A comparison of ResNet(m,d) with respect to parameters (m,d) in terms of accuracies, total number of parameters, and CPU time

(m,d)	RMSE	MAE	CPU time (s)	Parameters
(5,5)	1.71E-6	6.99E-4	1,258	163,901
(5,10)	2.46E-6	6.08E-4	1,696	308,301
(5,15)	2.28E-6	6.18E-4	2,050	452,701
(10,5)	8.18E-7	4.77E-4	1,1378	653,601
(10,10)	1.39E-6	6.57E-4	2,216	1,230,401
(10,15)	1.91E-6	5.63E-4	2,755	1,807,201

faces. Indeed, owing to gaps between the two materials, there are relatively small temperature drops in the embedded material, which coincides with the phenomena observed in [5].

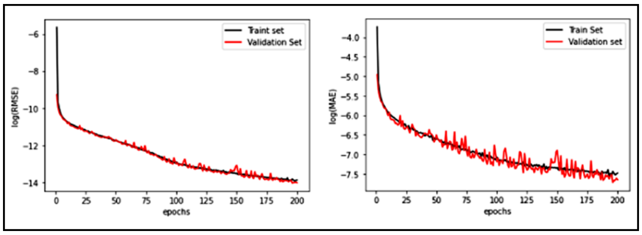

Fig. 2. Plots of evolutions of RMSE (left) and MAE (right) as the number of epochs increases.

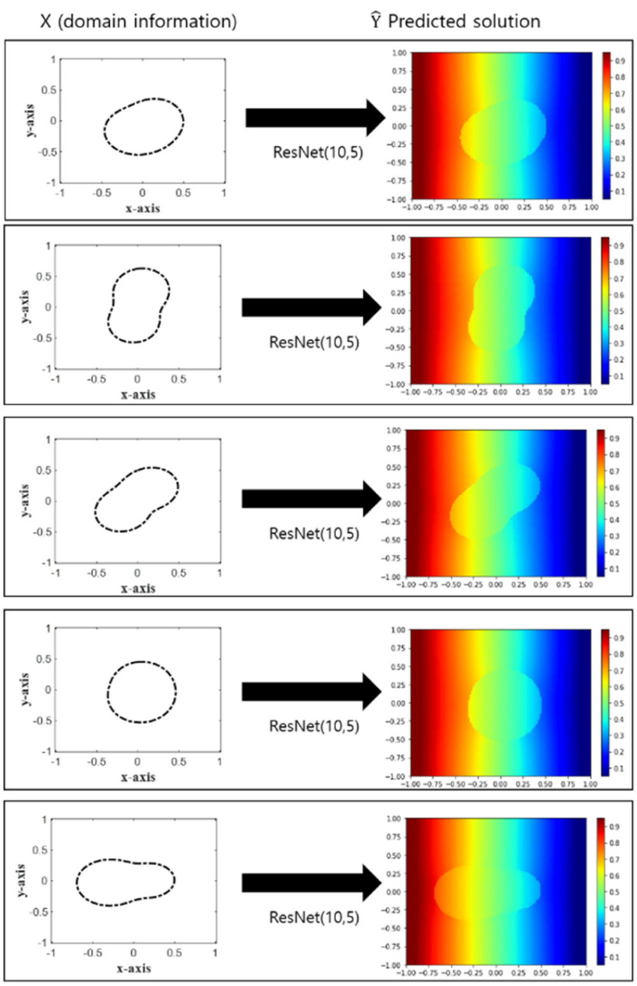

Fig. 3. Temperatures predicted by ResNet(10,5) with respect to different configurations of material subdomains are reported. The left column represents the shape of material-material interfaces and the right column shows the predicted temperature for each case.

V. CONCLUSION

In this study, we developed new algorithms to predict the solutions of heat-transfer models in composite materials. First, datasets were generated by solving heat-transfer equations numerically, and the IFEM was adopted for the implementation. To develop neural networks that are robust to the shapes of material subdomains, various geometries of material-material interfaces were considered in the datasets. Once the datasets were generated, we trained the ResNet-type neural networks, which we named ResNet(m,d). The results showed that the RMSEs were below 3E-6 and the MAEs were below 7E-4. In addition, the discontinuity of temperature variables were described by ResNet(m,d) in a reasonable manner.

ACKNOWLEDGMENT

The second author (G. Jo) was supported by the National Research Foundation of Korea (NRF) grant funded by the Korean government (MSIT) (No. 2020R1C1C1A01005396).

We would like to thank Editage (www.editage.co.kr) for English language editing.

REFERENCES

[1] C. -W. Nan and R. Birringer, “Effective thermal conductivity of particulate composites with interfacial thermal resistance,” *Journal of Applied Physics*, vol. 81, no. 10, pp. 6692-6699, Feb. 1997. DOI: 10.1063/1.365209.

[2] S. Torquato and M. D. Rintoul, “Effect of Interface on the Properties of Composite Media,” *Physical Review Letters*, vol. 75, no. 22, pp. 4067-4070, Dec. 1995. DOI: 10.1103/PhysRevLett.76.3241.

[3] P. L. Kapitza, “Heat transfer and superfluidity of helium II,” *Physical Revies*, vol. 60, no. 4, pp. 354-355, Aug. 1941. DOI: 10.1103/PhysRev.60.354.

[4] J. Yvonnet, Q. -C. He, and C. Toulemonde, “Numerical modelling of the effective conductivities of composites with arbitrarily shaped inclusions and highly conducting interface,” *Composites Science and Technology,* vol. 68, no. 13, pp. 2818-2825, Oct. 2008. DOI: 10.1016/j.compscitech.2008.06.008.

[5] J. Yvonnet, Q. -C. He, Q. -Z. Zhu, and J. -F. Shao, “A general and efficient computational procedure for modelling the Kapitza thermal resistance based on XFEM,” *Computational Material Science*, vol. 50, no. 4, pp. 1220-1224, Feb. 2011. DOI: 10.1016/j.commatsci.2010.02.040.

[6] G. Jo and D. Y. Kwak, “Enriched P1-conforming methods for elliptic interface problems with implicit jump conditions,” *Advances in Mathematical Physics*, Article ID: 9891281, Jun. 2018. DOI: 10.1155/2018/9891281.

[7] K. He, X. Zhang, S. Ren, and J. Sun, "Deep residual learning for image recognition," in *Proceedings of the IEEE conference on computer vision and pattern recognition*, Las Vegas: NV, USA, pp. 770-778, 2016. DOI: 10.1109/CVPR.2016.90.
[8] J. Lee, G. Wu, and H. Jung, "Deep learning document analysis system based on keyword frequency and section centrality analysis," *Journal of Information and Communication Convergence Engineering*, vol. 19, no. 1, pp. 48-53, Mar. 2021. DOI: 10.6109/jicce.2021.19.1.48.
[9] Y. Eom and J. Bang, "Speech emotion recognition using 2D-CNN with mel-frequency cepstrum coefficients," *Journal of Information and Communication Convergence Engineering*, vol. 19, no. 3, pp. 148-154, Sep. 2021. DOI: 10.6109/jicce.2021.19.3.148.
[10] Z. Wu, V. Lim, and H. Jung, "Customization using anthropometric data deep learning model-based beauty service system," *Journal of Information and Communication Convergence Engineering*, vol. 19, no. 2, pp. 73–78, Feb. 2021. DOI: 10.6109/JICCE.2021.19.2.73.
[11] G. Wang, K. -C. Lee, and S. -Y. Shin, "Novel image classification method based on few-shot learning in monkey species," *Journal of Information and Communication Convergence Engineering*, vol. 19, no. 2, pp. 79–83, Jun. 2021. DOI: 10.6109/JICCE.2021.19.2.79.
[12] I. Kwon, G. Jo, and K. -S. Shin, "A deep neural network based on ResNet for predicting solutions of poisson-boltzmann equation," *Electronics*, vol. 10, no. 21, pp. 2627, Oct. 2021. DOI: 10.3390/electronics10212627.
[13] D. Y. Kwak, S. Lee, and Y. Hyon, "A new finite element for interface problems having robin type jump," *International Journal of Numerical Analysis and Modeling*, vol. 14, no. 4, pp. 532-549, Aug. 2017.

Guangxing Wang
received his M.S. degree in Computer Application Technology from Huazhong University of Science and Technology, Wuhan, China in 2009. From 2016 to the present, he has been an associate professor in the Information Technology Center of Jiujiang University in China. received his M.S. and Ph.D. degrees from the Dept. of Computer Information Engineering of Kunsan National University, Gunsan, Korea, in 2018 and 2021, respectively. F His research interests Deep Learning, Image Processing, Diagnosis, etc.

Gwanghyun Jo
received his M.S. and Ph. D. degree in department of mathematical scient, KAIST in 2013 and 2018 respectively. From 2019 to the present, he has been a faculty member of the Department of Mathematics in Kunsan National University, Korea. His research interests include numerical analysis, computational fluid dynamics, machine learning.

Seong-Yoon Shin
received his M.S. and Ph.D. degrees from the Dept. of Computer Information Engineering of Kunsan National University, Gunsan, Korea, in 1997 and 2003, respectively. From 2006 to the present, he has been a professor in the same department. His research interests include image processing, computer vision, and virtual reality.